FNAL TD note # TD-06-040

April 23, 2006; last revision August 09, 2006

Solenoid Residual Magnetization Study

V.V. Kashikhin, I. Terechkine

I. Strand data

First test coils [1] were wound using SSC HEB dipole inner layer 0.808 mm NbTi strand that was provided by courtesy of LBNL's Ron Scanlan and Dan Dietderich. Because two versions of requirements for the strand existed and several firms participated in a bid for the strand fabrication, identifying the strand appeared not a straightforward task. After analyzing cross-section of the strand (Fig. 1), it was possible to find (by counting) the number of filaments in the strand: between 7500 and 8500. Filament diameter was evaluated by scaling, and was found to be ~6 μm.

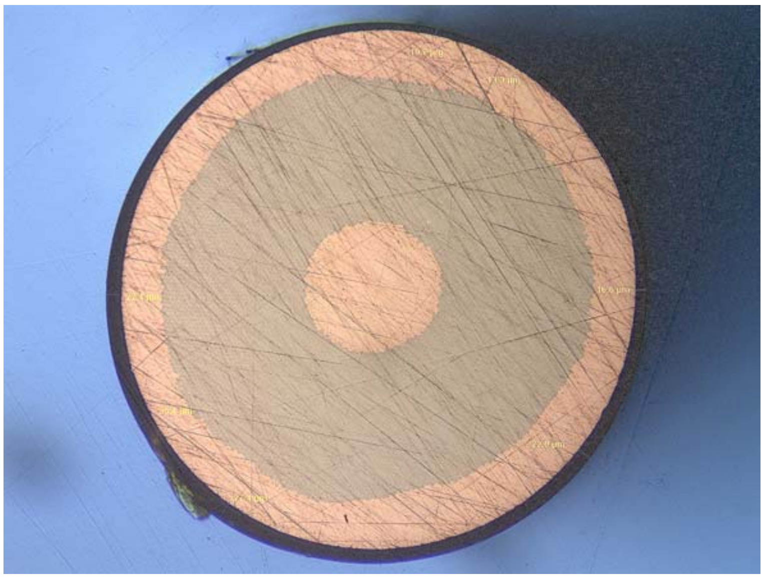

Fig. 1: Photo of the cross-section of the strand

As it was mentioned above, two sets of the requirements for the inner dipole strand round, 0.808 mm diameter) existed: the "old" (1986) and the "new" (1990). For the "old" specification [2], required filament diameter was ~ 5 μm with the total number of filaments in the strand of ~ 11,000. The specified ratio of Cu to non-Cu content was **1.3**. For the "new" specification [3], this ratio was **1.5**, the filament diameter requirement was ~ 6 μm, and the number of the filaments ~ 8000. The specified current for the "new" strand was 339 A at 7 T and 4.2 K. This is well compared, but slightly lower than the measured value (372 A) or the value used for magnetic modeling (350 A). The difference between the specified value and the measured one is ~ 10%. The "old" specification required 613 A current at 5 T; the measured value of the existing strand at 5 T was 640 A; the difference between the specified and the measured current was ~ 6%. So, based on the strand's current density it was difficult to come to a definite conclusion. Because the counted number of the filament and the measured filament diameter fitted the "new" specification, most probably, we used the "new" type of a strand. We will accept the existing strand parameters as following:

Cu/non-Cu = 1.5;

Strand diameter – 0.808 mm;

Number of filaments – 8000

Filament diameter – 6 μm;

The next table defines critical current as a function of the magnetic field at 4.2 K:

0 T	2200 A
3 T	900 A
5 T	640 A
7 T	370 A

There are two sources of residual magnetic field of the solenoid:

- magnetization of superconducting strand in the coil
- magnetization of the ferromagnetic yoke.

Impact of each of the sources is analyzed below.

II. Residual magnetization in the coil

Residual magnetization effect of hard superconducting material takes place due to existence of flux pinning centers that fix position of fluxoids inside the material. Magnetization is defined as a magnetic moment of the current per unit volume and for round strands it can be calculated as following [4]:

$$M = (2/3\pi)\cdot d_{eff}\cdot Ic/A$$

where d_{eff} is effective filament diameter, A is strand cross-section, and Ic is critical current of the strand (it is a function of magnetic field).

In the coil of a solenoid, magnetic field changes with the distance form the axis. It is maximal on the inner surface, quite small near the outer layer and can even have different sign there. So, the residual magnetization of strands in the solenoid is not uniform.

To estimate order of a magnitude of the effect, let's consider that the current in the solenoid is coming to zero after initially it was positive. We will accept also that each strand shows maximal magnetization with the magnetization vector in the direction of the initial central magnetic field (uniform magnetization approach). Fig.2 schematically compares magnetic field distribution during the cycle and after the current is set to zero.

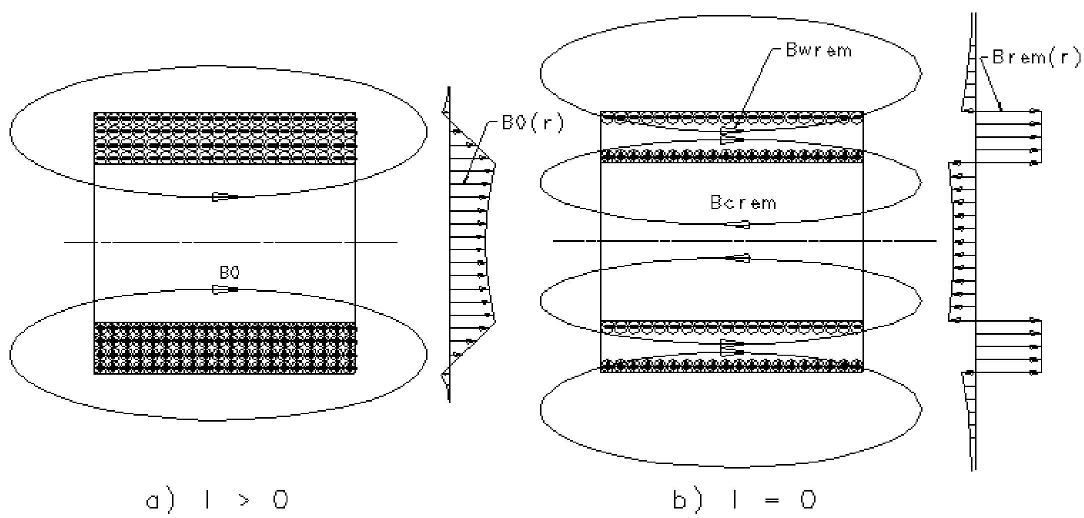

Fig. 2: Origin and direction of residual magnetic field inside the solenoid:

During the cycle (Fig. 2-a), there is magnetic field B0 in the center of the coil and in the winding. Most of the winding sees positive magnetic field. After the current is brought to zero (Fig. 2-b), direction of the residual magnetic field in the winding B_{wrem} remains as it was during the cycle (hysteretic effect). Strand magnetization is represented by two sheaths of current on the inner and on the outer surfaces of the coil. The total current in the coil is zero, but due to difference in the radii of the inner and the outer magnetization current sheaths, there is non-zero magnetic field in the winding and in the center of the coil. This combination of the currents results in the negative residual field B_{crem} in the center of the solenoid. The value of the field can be evaluated knowing the surface current density (or M) and the geometrical characteristics of the solenoid. The magnetic field in the center of a thin cylindrical layer of current

$$Bc = \mu 0 \cdot M \cdot \frac{L}{\sqrt{D^2 + L^2}}$$

where L is the length of the layer and D is the diameter. The field generated by two layers

$$Bc = -\mu 0 \cdot M \cdot L \cdot \left[\frac{1}{\sqrt{Din^2 + L^2}} - \frac{1}{\sqrt{Dout^2 + L^2}} \right]$$

The coil's inner diameter Din ≈ 60 mm, the outer diameter is Dout ≈ 92 mm, and the length L ≈ 100 mm. If Ic = 2200 A/mm^2 (B = 0), d_{eff} = 6 µm, and d_{str} = 0.808 mm, M = 5400 A/m and the value of the residual field in the center of the solenoid is -7.5 Gs. Results of modeling agree with the analytical approach (see Fig. 3 and Fig. 4).

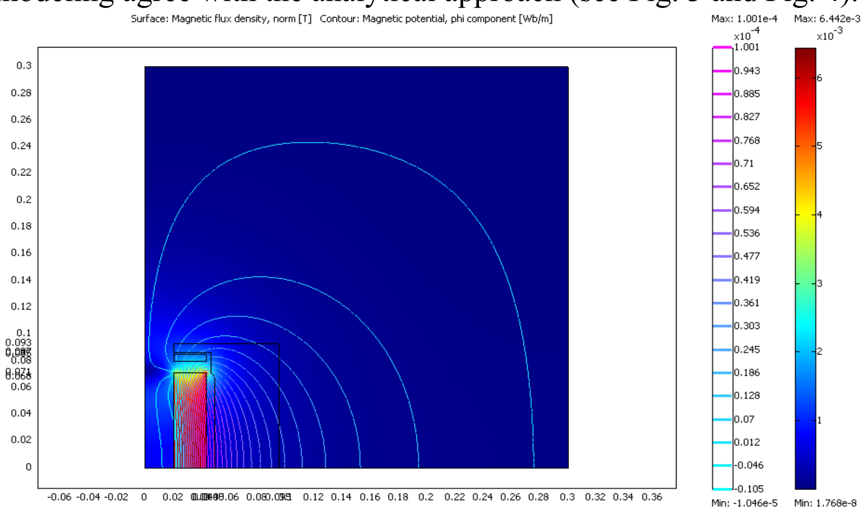

Fig. 3: Residual magnetization of the main coil with M = 5400 A/m

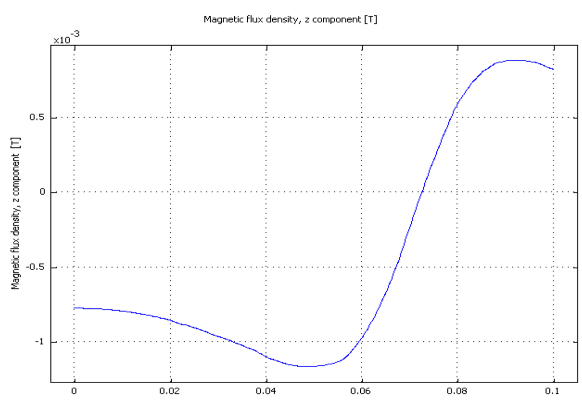

Fig. 4: Field distribution along z with M = 5400 A/m

For the Oxford strand, effective filament diameter d_{eff} = 70 μm and diameter of the strand d_{str} = 0.87 mm^2. Measured critical current density at B = 0 is 1767 A. Then residual magnetization of the strand is ~44000 A/m. This makes the residual field in the center of the magnet ~ 60 Gs. Modeling gives similar results.

More complex analysis involves t change of the magnetization direction due to the magnetic field vector rotation inside the coil. To understand this, let's take a look at the field lines of a simple solenoid without a flux return and without bucking coils (Fig. 5).

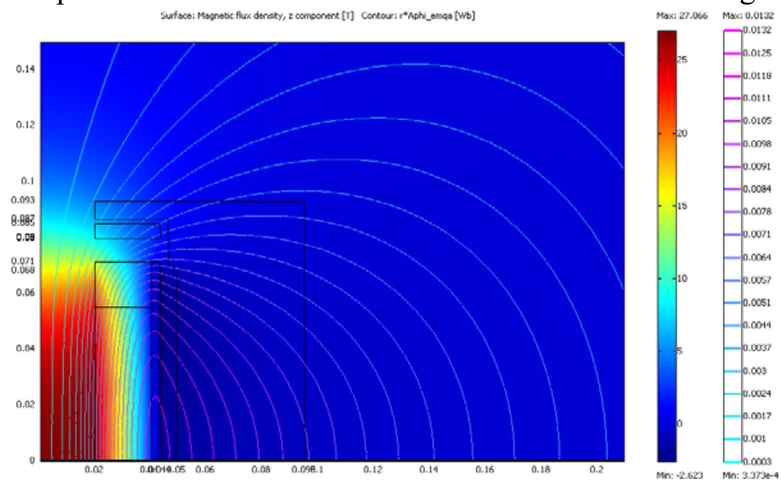

Fig. 5: Field lines of the main coil

Direction of the magnetic field in the body of the coil changes depending on the location of the point of interest: For the outer part of the coil (R = 40.5 – 43.5) it is mainly radial. For the end part of the coil (Z > 0.055), it is directed at the angle to the axis. The rest of the coil is magnetized mainly longitudinally. Fig. 6 below compares remnant field longitudinal distribution for different directions of magnetization of the end part of the coil (Oxford strand).

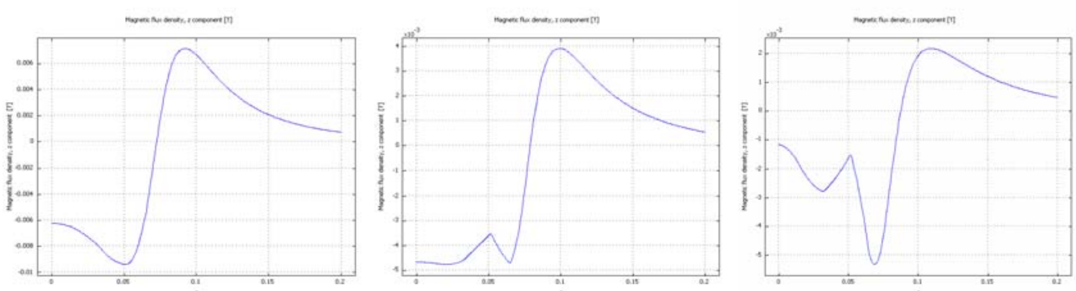

a) α = 0 deg   b) α = 30 deg   c) α = 45 deg

Fig. 6: Remnant magnetic field distribution depending on the direction of the residual magnetization of the end part of the coil

The shape of the curve inside the coil is somewhat sensitive to the direction of magnetization in the end part of the coil. Outside of the coil the remnant field distribution is not so sensitive to the details of the magnetization inside the coil.

For further analysis, we will accept the 45° direction of magnetization for the end parts of the main coil and radial magnetization for the bucking coils.

III. Magnetic field on the cavity wall due to residual magnetization of strands

If no bucking coils are present and no flux return is used, residual field distribution on the cavity wall is shown in Fig. 7.

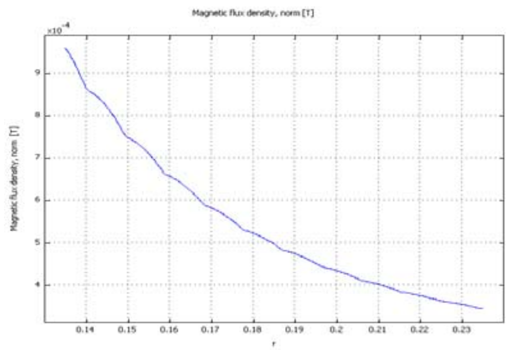

Fig. 7: Residual magnetic field on the cavity surface due to Oxford strand magnetization (**no bucking coils and no flux return**).

Magnetic field reaches ~ 10 Gs (10^{-3} T) as a result of residual magnetization.

Presence of a flux return brings fringe magnetic field on the wall to the level of ~2.6 μT (Fig. 8).

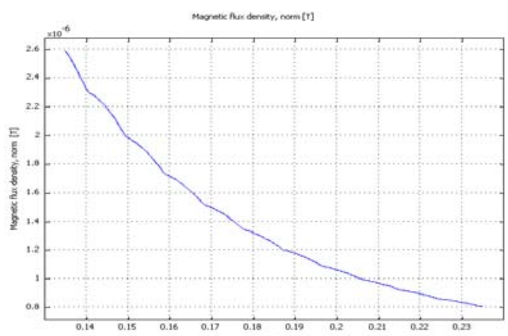

Fig. 8: Residual magnetic field on the cavity wall due to Oxford strand magnetization (**no bucking coils but there is a flux return**)

Use of bucking coil without a flux return does not provide needed degree of screening, as it is possible to see from Fig. 9 below; maximal field on the cavity wall still reaches ~ 10 Gs.

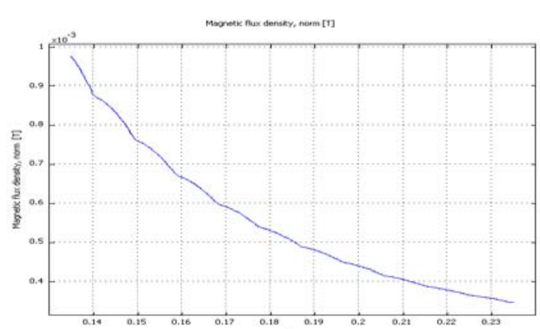

Fig. 9: Residual magnetic field on the cavity wall due to Oxford strand magnetization (**there are active bucking coils but there is no flux return**)

Adding the flux return again dramatically reduces the remnant field (Fig. 10).

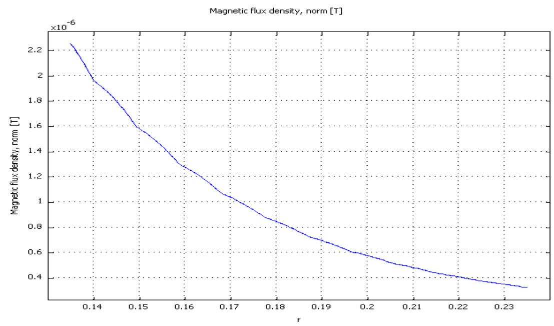

Fig. 10: Residual magnetic field on the cavity wall due to Oxford strand magnetization (**there are active bucking coils and a flux return**)

We can conclude at this point that presence of a flux return helps to significantly reduce remanent magnetic field (due to residual strand magnetization) on the cavity walls.

Similar conclusion was made for the solenoid wound using the SSC inner strand. For the bucking coils, 3 μm filament diameter was accepted. The analysis was performed using TOSCA modeling package with specially designed magnetization curve that took into the account specific features of superconducting strand magnetization [4]. Residual field distribution outside the solenoid is shown in Fig. 11 below. In the area of interest, the flux density was found to be ~ $5*10^{-7}$ T or about what one would get by scaling from the previous case taking into the account the difference in the filament size.

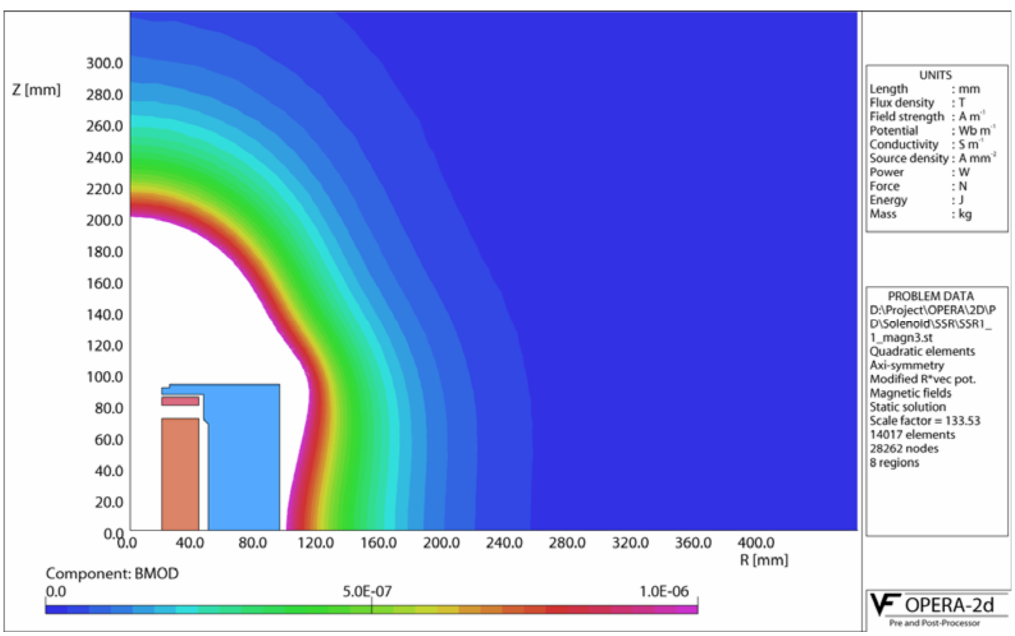

Fig. 11: Remnant flux density map (OPERA modeling results for SSC strand)

IV. Residual Magnetization of a Flux Return Material

To map residual fringe magnetic field which is due to the remanence in the flux return material, it is necessary to know values and directions of the residual magnetization in different parts of the flux return. Here we will evaluate this field by analyzing just two cases:

- uniform residual magnetization for whole volume of the flux return;
- magnetization of different parts of the yoke with fixed amplitude, but varying directions.

Fig. 12 compares residual field maps for the two cases, and from Fig. 13 on can get a quantitative comparison of the residual field on the cavity wall

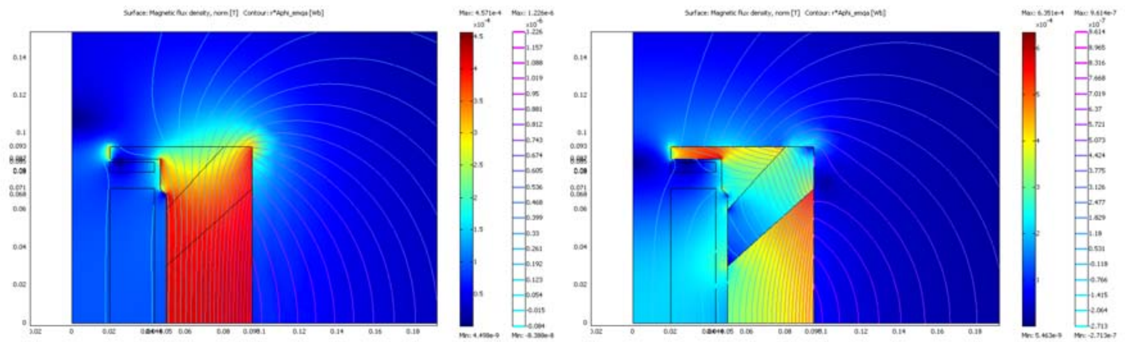

Fig. 12: Residual magnetic field map for different patterns of the residual magnetization

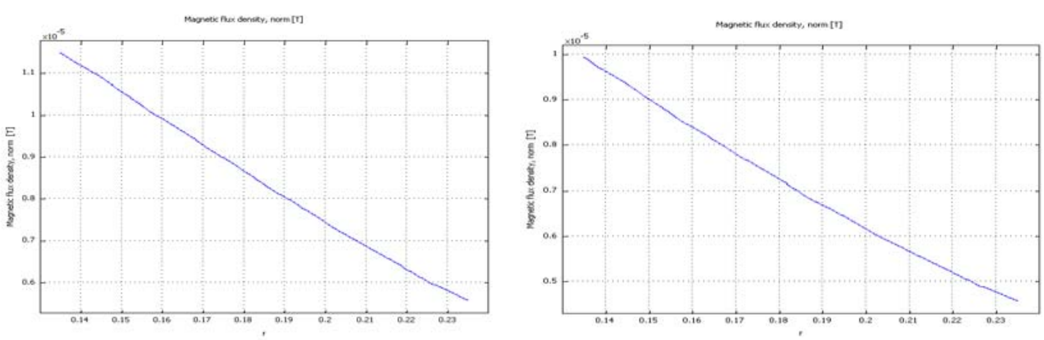

Fig. 13: Magnetic field on the cavity wall due to residual magnetization of the flux return

The residual field due to the flux return magnetization is on the level of ~ 0.1 Gs for both cases of magnetization pattern. This residual field will depend on quality of steel and post-fabrication heat treatment (annealing) of the yoke. For the modeling, residual magnetization was 400 A/m, which corresponds to ~ 5 Gs of coercive force and looks quite conservative (can happen though if the yoke steel quality is not good).

Although we've got quite encouraging results even with rather conservative steel properties, we can not rely on it fully because the material properties were taken at the room temperature. Magnetic properties of steel can become much more modest at LHe temperature. This issue requires additional study.

There are more reasons for the residual fringe magnetic field to grow, e.g. poor core assembly quality, uncertainties in the coil dimension, filament diameter, coil compaction factor, etc. To get low residual magnetic field, further reduction of the field can be reached by adding additional shielding. This issue is investigated in more details in [5].

V. Summary

1. The analysis of residual magnetization in the coil shows that this effect can be significant if no flux return is used;
2. Using good quality, annealed, low-carbon steel for the flux return helps to reduce the remnant magnetic field originated due to strand magnetization;
3. Residual magnetization of the steel flux return can result in significant increase of the remnant field;
4. One must know magnetic properties of material for a flux return at LHe temperature to get reliable modeling results.
5. Additional shielding is needed if the desired remnant field on the cavity walls is below ~ 100 mGs.

REFERENCES:

1. R Carcagno, et al, Test Solenoids: Expected Performance and Test Results, TD-06-027, TD-06-028, FNAL, July 2006
2. Conceptual Design of the SSC, SSC-SR-2020, March 1986, p. 280
3. SSC Site-Specific Conceptual Design, June 1990, p. 299
4. C. Boffo, Magnetization Measurements of Multifilamentary Superconducting Strands, Tesi de Laurea, FNAL, 1999
5. G. Davis, et al, SS-I Section Focusing Solenoid Prototype Cold Mass Design, TD-06-041, FNAL, August 2006